Dressed-molecule theory for the quasi-two-dimensional quantum anomaly

Fan Wu [1,*] Jian-shen Hu,[2,*] and Lianyi He[2]

[1]*Fujian Key Laboratory of Quantum Information and Quantum Optics, College of Physics and Information Engineering, Fuzhou University, Fuzhou, Fujian 350108, China*

[2]*Department of Physics and State Key Laboratory of Low-Dimensional Quantum Physics, Tsinghua University, Beijing 100084, China*

(Received 17 May 2023; revised 21 November 2023; accepted 11 December 2023; published 28 December 2023)

In this work the dressed-molecule theory is used to describe the two-dimensional quantum anomaly of breathing mode in a recent experimental system [M. Holten *et al.*, Phys. Rev. Lett. **121**, 120401 (2018); T. Peppler *et al.*, Phys. Rev. Lett. **121**, 120402 (2018)]. With the aid of a beyond-mean-field Gaussian pair fluctuation theory, we employ the dressed-molecule states to characterize the axial excited states and the Feshbach molecular states and propose a low-energy effective theory. We show that, in the whole crossover from a BCS superfluid to a Bose-Einstein condensate, our theory can describe the two-dimensional experimental systems precisely in the low-energy region. We explain the puzzling experimental observations of the smaller than expected breathing-mode frequency. Our establishment of the dressed-molecule theory for two-dimensional fermions can help in the understanding of the conformal anomaly in quasi-low-dimensional quantum systems.

DOI: 10.1103/PhysRevA.108.063318

I. INTRODUCTION

The study of the conformal anomaly in low-dimensional systems has received considerable attention in recent years. Due to the quantum effect, the symmetry of the classical theory can be destroyed; this is called a quantum anomaly. One of the best-known anomalies is the conformal anomaly, associated with the violation of scale invariance by quantum corrections or quantified in renormalization. Since renormalization or quantum corrections introduce a distance scale, the classically scale-invariant symmetry has been broken. This is ubiquitous in quantum field theory, such as quantum electrodynamics, quantum chromodynamics, and the Gross-Neveu model [1].

In the two-dimensional system, these quantum anomalies can be observed by measuring the breathing mode of two-component interacting Fermi gases [2,3]. The breathing-mode frequency has a weak dependence on the scattering length and deviates from the classical value $\omega_B = 2\omega_\perp$ within a range of 5%–10% [2,4,5]. Many previous articles predicted the observed quantum abnormal breathing mode from theoretical calculations and quantum Monte Carlo simulations [6–22]. However, two recent experimental results show that even in the deep two-dimensional region, the predicted results are still quite different from the experimental data [21,22]. The observed frequency is far lower than the well-established theoretical prediction in the strong-interaction region [2,4].

The purpose of this work is to provide a different theory of the quasi-two-dimensional quantum anomaly to explain the experimental observations of the quantum anomaly of the breathing-mode frequency. In a previous work we established a minimal model to describe ultracold interacting fermions confined in two dimensions and solved it at zero temperature with the help of existing auxiliary-field quantum Monte Carlo results [23]. In the BCS superfluid region, this minimal model resolves to a certain extent the puzzling experimental observations of the smaller than expected equations of state and breathing-mode frequency. However, the agreement between the theoretical calculation and experimental data becomes worse in the Bose-Einstein condensate (BEC) region, suggesting the inadequacy of our theory towards the limit of a BEC. This makes it necessary to put forward an alternative theory to describe the two-dimensional interaction ultracold fermions in the experimental system with the whole BCS-BEC crossover. An alternative theory to explain experimental observations needs to meet the following conditions. First, this theory must be able to characterize the quantum anomaly of the breathing-mode frequency, so it must be a beyond-mean-field theory. Second, because of the strong-interaction region, the energy of the z-axis potential cannot always be much larger than other energy index scales. This means the axial excited-state fermion effect cannot be neglected. Finally, in the BEC region, the properties of the Feshbach molecular states will be dominant.

In this work, by using the Gaussian pair fluctuation theory to describe the quantum properties of the system and employing the dressed-molecule states [24] to characterize the axial excited states and the Feshbach molecular states, we develop an alternative theory. We show that, in the whole crossover from a BCS superfluid to a BEC, our theory can describe the two-dimensional experimental systems more precisely in the low-energy region. The paper is organized as follows. In Sec. II we establish the dressed-molecule model by fitting the two-body parameters with the two-channel model of the three-dimensional experimental system. We also verify the completeness of this model in the whole BCS-BEC crossover. In Sec. III we formulate the many-body theory of

*These authors contributed equally to this work.

the dressed-molecule model and give the calculation method of the breathing-mode frequency. In Sec. IV we show the results of the many-body calculations. We summarize in Sec. V.

II. DRESSED-MOLECULE MODEL

A. System description

In order to obtain a different theory describing the quasi-two-dimensional quantum anomaly, we need to get an effective model that can characterize the few-body physics of the quasi-two-dimensional system. So first we focus on the two-body problem in the three-dimensional two-component Fermi gases with s-wave interaction by a one-dimensional z-directional harmonic trap. This two-body Hamiltonian is taken in the two-channel form

$$\begin{aligned} H &= H_0 + H_{\rm bf} + H_{\rm int}, \\ H_0 &= \sum_{\sigma=\uparrow,\downarrow} \int d^3\boldsymbol{r}\, \psi_\sigma^\dagger \left(-\frac{\hbar^2\nabla^2}{2m_f} + \frac{1}{2}m_f\omega_z^2 z^2\right)\psi_\sigma \\ &\quad + \int d^3\boldsymbol{r}\, \phi^\dagger \left(-\frac{\hbar^2\nabla^2}{4m_f} + m_f\omega_z^2 z^2 + \bar{\nu}_b\right)\phi, \\ H_{\rm bf} &= \bar{g}_b \int d^3\boldsymbol{r}(\phi^\dagger\psi_\downarrow\psi_\uparrow + \text{H.c.}), \\ H_{\rm int} &= \bar{U}_b \int d^3\boldsymbol{r}\, \psi_\uparrow^\dagger\psi_\downarrow^\dagger\psi_\downarrow\psi_\uparrow, \end{aligned} \tag{1}$$

where ψ_σ and ϕ are the atomic and molecular field operator, ω_z is the trap frequency of the z-directional harmonic trap, and $\bar{\nu}_b$, $\bar{g}_b$, and $\bar{U}_b$ are the bare detuning, the bare atom-molecule coupling constant, and the bare background scattering amplitude, respectively. These bare scattering parameters are related to the physical ones (just like $\bar{U}_p$) via the renormalization relations [25]

$$\begin{aligned} U_c^{-1} &= -\int \frac{d^3\boldsymbol{k}}{(2\pi^3)}\frac{1}{2\bar{\epsilon}_{\boldsymbol{k}}}, \quad \Gamma^{-1} = 1 + \frac{U_p}{U_c}, \\ U_p &= \Gamma^{-1}\bar{U}_b, \quad g_p = \Gamma^{-1}\bar{g}_b, \quad \nu_p = \bar{\nu}_b + \Gamma\frac{g_p^2}{U_c}. \end{aligned} \tag{2}$$

The physical parameters are determined from the scattering data as

$$\begin{aligned} U_p &= \frac{4\pi\hbar^2 a_{\rm bg}}{m_f}, \quad g_p = \sqrt{\frac{4\pi\hbar^2\mu_{\rm co}W|a_{\rm bg}|}{m_f}}, \\ \nu_p &= \mu_{\rm co}(B - B_0), \end{aligned} \tag{3}$$

where $a_{\rm bg}$ is the background scattering length, W is the resonance width, $\mu_{\rm co}$ is the difference in the magnetic moments of the closed and open channels, and B_0 is the resonance position.

To better understand this Hamiltonian, we use harmonic modes and plane waves to expand the field operators in the trapped z direction and the untrapped x-y plane. Here we consider just the center of mass as the zero case as it is decoupled from the relative momentum in the two-body case. The Hamiltonian is taken as

$$\begin{aligned} H_0 &= \sum_{m,\mathbf{k},\sigma} \epsilon_{m,\mathbf{k}} c_{m,\mathbf{k},\sigma}^\dagger c_{m,\mathbf{k},\sigma} + \nu_b b_0^\dagger b_0, \\ H_{\rm bf} &= g_b \sum_{m,n,\mathbf{k}} \gamma_{mn}(b_0^\dagger c_{m,-\mathbf{k},\downarrow} c_{n,\mathbf{k},\uparrow} + \text{H.c.}), \\ H_{\rm int} &= U_b \sum_{m,n,\mathbf{k},m',n',\mathbf{k}'} c_{m,\mathbf{k},\uparrow}^\dagger c_{n,-\mathbf{k},\downarrow}^\dagger c_{n',-\mathbf{k}',\downarrow} c_{m',\mathbf{k}',\uparrow}. \end{aligned} \tag{4}$$

Here the Hamiltonian is the dimensionless Hamiltonian with the energy unit $E_0 = \hbar\omega_z$ and the length unit $a_t = \sqrt{\hbar/m_f\omega_z}$. The bosonic field b_0 represents the molecular state with transverse momentum $k = 0$ and axial harmonic mode $m = 0$. The atomic relative energy $\epsilon_{m,\mathbf{k}} = \frac{1}{4} + m + k_x^2 + k_y^2$. For the coefficient γ_{mn}, when $m + n$ is odd, $\gamma_{mn} = 0$; when $m + n$ is even,

$$\gamma_{mn} = \frac{(-1)^{(m-n)/2}}{(2\pi^3)^{1/4}\sqrt{m!n!}}\Gamma\left(\frac{m+n+1}{2}\right). \tag{5}$$

For the bare parameter, $g_b = \bar{g}_b a_t^{-3/2}/\hbar\omega_z$, $U_b = \bar{U}_b a_t^{-3}/\hbar\omega_z$, and $\nu_b = \bar{\nu}_b/\hbar\omega_z$.

We find that, in the Hamiltonian (4), there are three types of states: fermions in the axial ground state, fermions in axial excited states, and Feshbach molecular states. In order to fully characterize these states, we use the two-dimensional (2D) dressed-molecule model. It is a two-channel model in which the particles in the open channel are fermions, representing the fermions in the axial ground state, and the particles in the closed channel are the dressed bosons, representing the fermions in axial excited states and the Feshbach molecules [24,26–30]. This effective Hamiltonian is also written in dimensionless form with length unit a_t and energy unit $\hbar\omega_z$:

$$\begin{aligned} H_{\rm eff} &= \sum_{\mathbf{k},\sigma} \epsilon_{\mathbf{k}} a_{\mathbf{k},\sigma}^\dagger a_{\mathbf{k},\sigma} + \sum_{\mathbf{q}} (\delta_b + \epsilon_{\mathbf{q}}/2) d_{\mathbf{q}}^\dagger d_{\mathbf{q}} \\ &\quad + \alpha_b \sum_{\mathbf{k},\mathbf{q}} (d_{\mathbf{q}}^\dagger a_{\mathbf{k}+\mathbf{q}/2,\uparrow} a_{-\mathbf{k}+\mathbf{q}/2,\downarrow} + \text{H.c.}) \\ &\quad + V_b \sum_{\mathbf{k},\mathbf{k}',\mathbf{q}} a_{\mathbf{k}+\mathbf{q}/2,\uparrow}^\dagger a_{-\mathbf{k}+\mathbf{q}/2,\downarrow}^\dagger a_{-\mathbf{k}'+\mathbf{q}/2,\downarrow} a_{\mathbf{k}'+\mathbf{q}/2,\uparrow}. \end{aligned} \tag{6}$$

Here $\epsilon_{\mathbf{k}} = k^2/2$; δ_b, α_b, and V_b are the three bare scattering parameters; $a_{\mathbf{k},\sigma}^\dagger$ ($a_{\mathbf{k},\sigma}$) are fermionic creation (annihilation) operators; and $d_{\mathbf{q}}^\dagger$ ($d_{\mathbf{q}}$) are bosonic creation (annihilation) operators. Here the dressed molecules are structureless, because all short-range details associated with the fermions in axial excited states and the Feshbach molecules are irrelevant in the low-energy region. The bare scattering parameters can be linked to physical ones by use the 2D renormalization analogous to Eq. (2):

$$\begin{aligned} V_c^{-1} &= -\int \frac{d^2\boldsymbol{k}}{4\pi^2}\frac{1}{2\bar{\epsilon}_{\boldsymbol{k}} + 1}, \quad \Omega^{-1} = 1 + \frac{V_p}{V_c}, \\ V_p &= \Omega^{-1}V_b, \quad \alpha_p = \Omega^{-1}\alpha_b, \quad \delta_p = \delta_b + \Omega\frac{\alpha_p^2}{V_c}. \end{aligned} \tag{7}$$

B. Parameter fitting

Here we set the physical scattering parameters in the dressed-molecule model. To ensure the low-energy efficiency

of the dressed-molecule model, we use the T matrix as the benchmark to do the parameter fitting.

From the Hamiltonian (4) we can get the T matrix of the three-dimensional system

$$T_{3D}(E_{3D})^{-1} = \sqrt{2\pi}\left[\left(U_p - \frac{g_p^2}{\nu_p - E_{3D}}\right)^{-1} - S_p(E_{3D})\right]. \tag{8}$$

Here $S_p(E_{3D})$ is the two-particle bubble function of the system. We can get it by solving the two-body bound-state equation with the general two-body state ansatz involving the atoms and the molecule. The two-particle bubble function is

$$\begin{aligned} S_p(E_{3D}) &\equiv \sum_{m,n,\mathbf{k}} \gamma_{mn}^2 \left(\mathcal{E}_{m,n,\mathbf{k}}^{-1} + \frac{1}{2\epsilon_{\mathbf{k}}}\right) \\ &= \frac{-1}{4\sqrt{2}\pi} \int_0^{+\infty} ds \left(\frac{\Gamma(s+\frac{1}{4} - E_{3D}/2)}{\Gamma(s+\frac{3}{4} - E_{3D}/2)} - 1/\sqrt{s}\right), \end{aligned} \tag{9}$$

where $\mathcal{E}_{m,n,\mathbf{k}} = E_{3D} - k^2 - 1 - m - n$ and E_{3D} is the energy of the two-body system in the Hamiltonian (4). This is equivalent to the quasi-2D bubble function calculated by Petrov and Shlyapnikov [31], the details of which are given in the Appendix. Similarly, for the Hamiltonian (6) of the dressed-molecule model, the T matrix and the two-particle bubble function are

$$T_{2D}(E_{2D})^{-1} = \left(V_p - \frac{\alpha_p^2}{\delta_p - E_{2D}}\right)^{-1} - \sqrt{2\pi}\sigma_p(E_{2D}), \tag{10}$$

$$\begin{aligned} \sigma_p(E_{2D}) &= \int \frac{d^2\mathbf{k}}{(2\pi)^{5/2}} \left(\frac{1}{E_{2D} - 2\epsilon_{\mathbf{k}}} + \frac{1}{1 + 2\epsilon_{\mathbf{k}}}\right) \\ &= \frac{\ln(-E_{2D})}{4\pi\sqrt{2\pi}}, \end{aligned} \tag{11}$$

where E_{2D} is the energy of the two-body system in the dressed-molecule model.

Now we do the parameter fitting. First, from Eqs. (4) and (6) for the vacuum state, the energy of the vacuum state in the quasi-two-dimensional Hamiltonian is $E_{3D} = \frac{1}{2}$; for the dressed-molecule model it is $E_{2D} = 0$. So we can get $E_{3D} = E_{2D} + \frac{1}{2}$. For convenience, we define the two-body energy as $E = E_{2D}$.

Second, we consider the $\nu_p \to \infty$ case. We define E_b^{inf} as the bounding energy in the dressed-molecule model with $\nu_p \to \infty$. We obtain

$$U_p^{-1} = S_p\left(E_b^{\text{inf}} + \tfrac{1}{2}\right). \tag{12}$$

From this equation we can solve the bounding energy E_b^{inf} and we also have $V_p^{-1} = \sqrt{2\pi}\sigma_p(E_b^{\text{inf}})$. We define $C_p = S_p(E_b^{\text{inf}} + \frac{1}{2}) - \sigma_p(E_b^{\text{inf}})$ and then we can fit the parameter V_p by the equation

$$V_p^{-1} = \sqrt{2\pi}\left(U_p^{-1} - C_p\right). \tag{13}$$

Third, we know that the T matrix has simple poles when E is equal to a two-body bound state of the Hamiltonian. By matching the pole of the T matrix in Eqs. (8) and (10), we get

$$\left(V_p - \frac{\alpha_p^2}{\delta_p - E_b}\right)^{-1} = \sqrt{2\pi}\sigma_p(E_b). \tag{14}$$

Here E_b is the solution of the equations $U_{\text{eff}}(E)^{-1} = S_p(E + \frac{1}{2})$ and $U_{\text{eff}}(E) = U_p - g_p^2/[\nu_p - (E + \frac{1}{2})]$. By matching the first derivative of T^{-1} around the pole, we get

$$\begin{aligned} \frac{\partial}{\partial E_b} V_{\text{eff}}(E_b)^{-1} = \frac{\sqrt{2\pi}\partial}{\partial E_b}\Big[&U_{\text{eff}}(E_b)^{-1} \\ &- S_p\left(E_b + \frac{1}{2}\right) + \sigma_p(E_b)\Big], \end{aligned} \tag{15}$$

where $V_{\text{eff}}(E_b) = V_p - \alpha_p^2/(\delta_p - E_b)$. Then we can fit the parameters δ_p and α_p by the equations

$$\begin{aligned} \delta_p &= E_b - \frac{\sigma_p(E_b)\Lambda(E_B)}{\frac{\partial}{\partial E_b}\left[U_{\text{eff}}(E_b)^{-1} - S_p\left(E_b + \frac{1}{2}\right) + \sigma_p(E_b)\right]}, \\ \alpha_p^2 &= \frac{\Lambda(E_B)^2}{\sqrt{2\pi}\frac{\partial}{\partial E_b}\left[U_{\text{eff}}(E_b)^{-1} - S_p\left(E_b + \frac{1}{2}\right) + \sigma_p(E_b)\right]}, \end{aligned} \tag{16}$$

where $\Lambda(E_B) = [1 - \sigma_p(E_b)/(U_p^{-1} - C_p)]$.

In Fig. 1 we plot the parameters of the dressed-molecule model responding to the quasi-two-dimensional system [21]. Here V_{eff} is the effective interaction defined before; it will play an important role in the many-body calculation discussed below. The horizontal axis parameter a_s is the effective 2D scattering length $a_s \equiv a_z\sqrt{\pi/\mathcal{B}}\exp -\sqrt{\pi/2}a_z/a_{3D}$, with $a_{3D} = (U_p - g_p^2/\nu_p)/4\pi$ and $\mathcal{B} \sim 0.905$ [31]. We also show the effective range of the dressed-molecule model in Fig. 2; compared to the effective theory in our previous article [23], the properties of the two curves with an effective range are consistent. However, as the parameter approaches the BEC limit, the difference between these two curves begins to appear. This occurs, on the one hand, because the model for the effective theory in our previous work is a concise model, but the dressed-molecule model is a better model in the low-energy region. On the other hand, in this paper, the three-dimensional Hamiltonian is described in the two-channel form, so on the BEC side, this description is more physical than that in our previous work [23].

We have introduced an effective dressed-state 2D Hamiltonian by matching the two-body physics with three-dimensional systems. This effective theory is a better model in the low-energy region. By grouping the axial excited-state fermions and Feshbach molecules to define a dressed-molecule state, we can keep the correction of the low-energy many-body physics. Because of the matching conditions of the pole of the two-body T matrix and the first derivative of T^{-1} around the pole, when the fermionic chemical potential is not far away from the bound-state energy, just $|2\mu + |E_b|| \ll 1$, the T matrix of the three-dimensional Hamiltonian can be well approximated by that of the dressed-molecule model. Considering the fact that $|2\mu + |E_b|| \leqslant E_F$ through the BCS-BEC crossover, where E_F is the Fermi energy and the Fermi energy is proportional to the number density $E_F \propto n$, for the diluteness and the quasi-2D systems we consider in this paper, this effective dressed-state theory is approximately valid. This

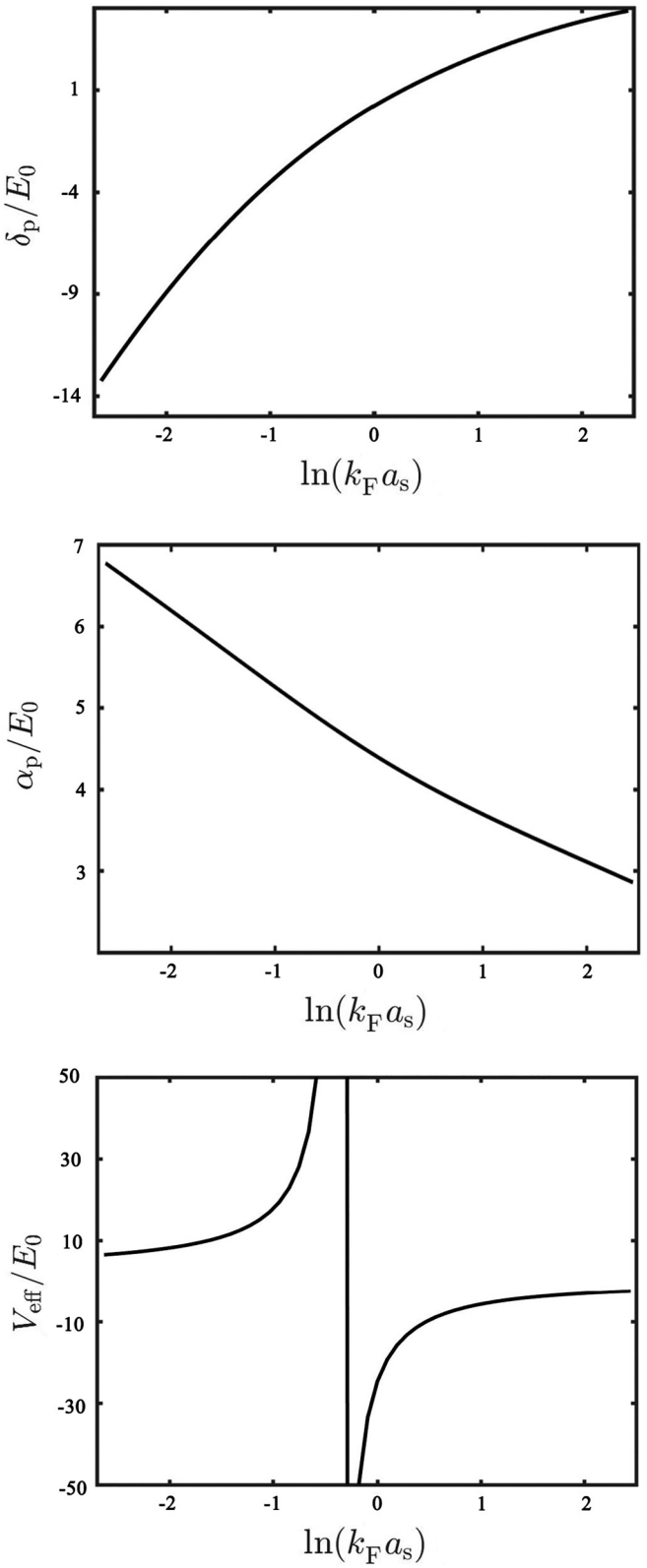

FIG. 1. Evolution curve of the two-body interaction parameters in the dressed-molecule model with the change of $\ln(k_F a_s)$. Here δ_p is the effective energy difference between open and closed channels, α_p is the effective coupling strength between open and closed channels, V_{eff} is the effective interaction strength, and the unit of the two-body interaction parameters $E_0 = \hbar\omega_z$.

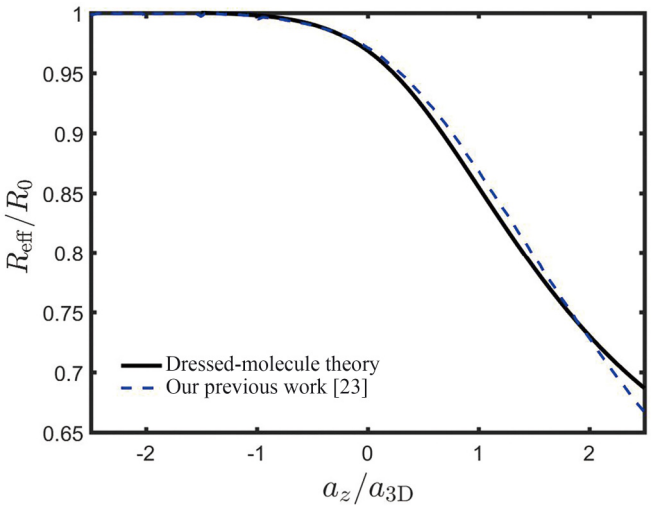

FIG. 2. Effective 2D effective range R_{eff} change with the 3D interaction strength a_z/a_{3D}. Here the unit of R_{eff} is the 2D effective range in the BCS limit $R_s^{(0)} = (-\ln 2)a_z^2$. The black solid line is the result of our dressed-molecule theory and the blue dotted line is the data of our previous work [23].

is also the reason why we overlooked the impact of the closed-channel molecules beyond the ground state in our model.

III. GAUSSIAN PAIR FLUCTUATION THEORY

We carry out the many-body simulation based on this dressed-molecule model. Through Eq. (6), in the imaginary-time path-integral formalism, the partition function $\mathcal{Z}$ is given by

$$Z = \int \mathfrak{D}[\Psi_\sigma^\dagger, \Psi_\sigma, \Phi^\dagger, \Phi] e^{-\mathcal{S}_{\text{eff}}[\Psi_\sigma^\dagger, \Psi_\sigma, \Phi^\dagger, \Phi]}, \tag{17}$$

where Ψ_σ and Φ are the real-space atomic and molecular field operators corresponding to $a_{\mathbf{k},\sigma}$ and $d_{\mathbf{q}}$ in Eq. (6) and S_{eff} is the effective action

$$\begin{aligned}\mathcal{S}_{\text{eff}}[\Psi_\sigma^\dagger, \Psi_\sigma, \Phi^\dagger, \Phi] &= \int_0^\beta d\tau \Bigg\{ \int \frac{d^2\boldsymbol{r}}{S} \Bigg[\Psi_\sigma^\dagger(\boldsymbol{r}) \left(\frac{\partial}{\partial\tau} - \mu \right) \Psi_\sigma(\boldsymbol{r}) \\ &\quad + \Phi^\dagger(\boldsymbol{r}) \left(\frac{\partial}{\partial\tau} - 2\mu \right) \Phi(\boldsymbol{r}) \Bigg] + H_{\text{eff}} \Bigg\}. \end{aligned} \tag{18}$$

Here τ is the imaginary time after the replacement $t \to -i\tau$, $\beta = 1/k_B T$ is the inverse temperature, and the effective Hamiltonian H_{eff} is the real-space form of Eq. (6). Through the Gaussian integral, fermions can be directly integrated out and we obtain

$$Z = \int \mathfrak{D}[\Delta^\dagger, \Delta] e^{-\mathcal{S}_{\text{eff}}[\Delta^\dagger, \Delta]}, \tag{19}$$

$$\mathcal{S}_{\text{eff}}[\Delta^\dagger, \Delta] = -\int dx\, \Delta^\dagger \frac{1}{\mathcal{V}_{\text{eff}}} \Delta \; - \; \text{Tr} \ln G^{-1}[\Delta, \Delta^\dagger], \tag{20}$$

where $x = (\tau, \mathbf{r})$, $\int dx = \int_0^\beta d\tau \int d\mathbf{r}$, and $\Delta = \alpha_b \Phi + V_b \Psi_\downarrow \Psi_\uparrow$ is the auxiliary field. By Fourier transforming,

the effective action can be written in the momentum space with dimensionless form (length unit a_t and energy unit $\hbar\omega_z$). Then we can get $\mathcal{V}_{\rm eff} \to V_{\rm eff}(iq_l, \mathbf{q}) = V_p - \alpha_p^2/(-iq_l + \mathbf{q}^2/4 + \delta_p - 2\mu)$ and the fermion matrix

$$G^{-1}[\Delta, \Delta^\dagger] = \begin{pmatrix} i\omega_n - \xi_k & \Delta \\ \Delta^\dagger & i\omega_n + \xi_k \end{pmatrix}. \tag{21}$$

In the mean-field level at zero temperature $\Delta(x) = \Delta_0 = \alpha_b\langle d_0\rangle + V_b\sum_{\mathbf{k}}\langle a_{-\mathbf{k},\downarrow}a_{\mathbf{k},\uparrow}\rangle$, the grand potential $\Omega = -(T/V)\ln\mathcal{Z}$ can be evaluated as

$$\Omega_{\rm MF} = -\frac{\Delta_0^2}{V_{\rm eff}(0,0)} + \sum_{\mathbf{k}}\left(\xi_{\mathbf{k}} - E_{\mathbf{k}} + \frac{\Delta_0^2}{k^2+1}\right), \tag{22}$$

where $\xi_{\mathbf{k}} = k^2/2 - \mu$ and $E_{\mathbf{k}} = \sqrt{\xi_{\mathbf{k}}^2 + \Delta^2}$. However, the mean-field theory is not enough to describe the quantum anomaly, and the quantum fluctuation in the system cannot be ignored. To have a more quantitative description, we consider quantum fluctuations around the saddle point by writing $\Delta(x) = \Delta_0 + \eta(x)$. An exact analytical treatment of the fluctuation contribution is impossible. In our theory, we use the Gaussian pair fluctuation approximation to calculate the quantum fluctuation [32,33]. The fluctuation grand potential can be written as

$$\Omega_{\rm GF} = \sum_{q,iq_l}\ln M_{11} + \frac{1}{2}\ln\left(1 - \frac{M_{12}^2}{M_{11}M_{22}}\right). \tag{23}$$

While using the renormalization condition, we express M_{11} and M_{12} as

$$M_{11} = -\frac{1}{V_{\rm eff}(iq_l,\mathbf{q})} + \frac{1}{2}\sum_{\mathbf{k}}\left\{\frac{2}{k^2+1} - \left[\left(1 + \frac{\xi_{\mathbf{k}}}{E_{\mathbf{k}}}\frac{\xi_{\mathbf{k}+\mathbf{q}}}{E_{\mathbf{k}+\mathbf{q}}}\right)\frac{E_{\mathbf{k}} + E_{\mathbf{k}+\mathbf{q}}}{(E_{\mathbf{k}} + E_{\mathbf{k}+\mathbf{q}})^2 + q_l^2} - \left(\frac{\xi_{\mathbf{k}}}{E_{\mathbf{k}}} + \frac{\xi_{\mathbf{k}+\mathbf{q}}}{E_{\mathbf{k}+\mathbf{q}}}\right)\frac{iq_l}{(E_{\mathbf{k}} + E_{\mathbf{k}+\mathbf{q}})^2 + q_l^2}\right]\right\}, \tag{24}$$

$$M_{12} = \frac{1}{2}\sum_{\mathbf{k}}\frac{\Delta^2}{E_{\mathbf{k}}E_{\mathbf{k}+\mathbf{q}}}\frac{E_{\mathbf{k}} + E_{\mathbf{k}+\mathbf{q}}}{(E_{\mathbf{k}} + E_{\mathbf{k}+\mathbf{q}})^2 + q_l^2}. \tag{25}$$

In this work we use the local-density approximation and adopt the commonly used sum-rule method to calculate the breathing-mode frequency [4,34]. Due to the neglect of the influence of highly excited states in the breathing mode in this sum-rule approach, it can only give the upper bound of the breathing-mode frequency. When the total particle number is fixed, the relation between the total particle number and particle density can naturally be written as

$$\mu = \mu_c - \tfrac{1}{2}m_f\omega_\perp^2 r^2, \tag{26}$$

$$N = \int_0^\infty d\mathbf{r}\, n(\mu). \tag{27}$$

Here $\omega_\perp$ is the trap frequency of the harmonic trap in the transverse direction and m_f is the mass of the fermion. By using the sum-rule approach [35,36], we can calculate the breathing mode at zero temperature

$$\hbar^2\omega_B^2 = -2\langle r^2\rangle\left(\frac{d\langle r^2\rangle}{d(\omega_\perp^2)}\right)^{-1}, \tag{28}$$

where $\langle r^2\rangle = N^{-1}\int_0^\infty d\mathbf{r}\, r^2 n(\mu)$. Finally, we find the relation between the ground-state energy in the center of the potential and the particle number

$$\Omega_{\rm MF} + \Omega_{\rm GF} = -\frac{Nm_f\omega_\perp^2}{2\pi}. \tag{29}$$

IV. MANY-BODY CALCULATION RESULTS

Now we focus on the many-body calculation results. First, we focus on the results of the region near the resonance point. In Fig. 3 we plot the breathing-mode frequency change with the number of the fermions in the trap compared to the experimental data at $\ln(k_F a_s) \sim -0.1$ [21]. Due to the fact that the temperature in these two experiments almost meet the requirement of being much lower than the Fermi temperature, we have neglected the temperature effect in the experiment and directly compared it with our zero-temperature calculation. The equation-of-state calculation of the quantum Monte Carlo (QMC) at this point is quite different from the experimental data even for $N/N_{\rm 2D} = 0.2$ [37]. Because of that, when $\ln(k_F a_s) \sim -0.1$, the corresponding effective strength of the interaction $V_{\rm eff}/\hbar\omega_z \sim -15$ (see Fig. 1), which exceeds

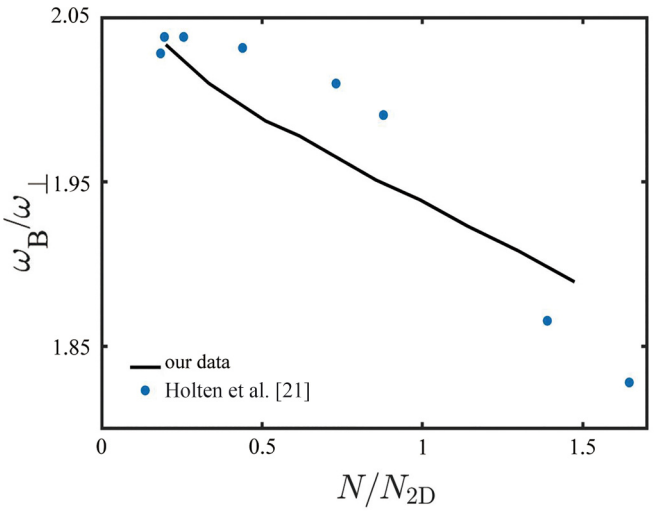

FIG. 3. Breathing-mode frequency change with the number of the fermions in the trap. The black solid line is the result of our dressed-molecule theory and the blue dots are the experimental data of Holten *et al.* at $0.10 \sim 0.18T_F$ [21]. Here $N_{\rm 2D} \simeq (\omega_z/\omega_\perp)^2$ is the 2D threshold for an ideal gas.

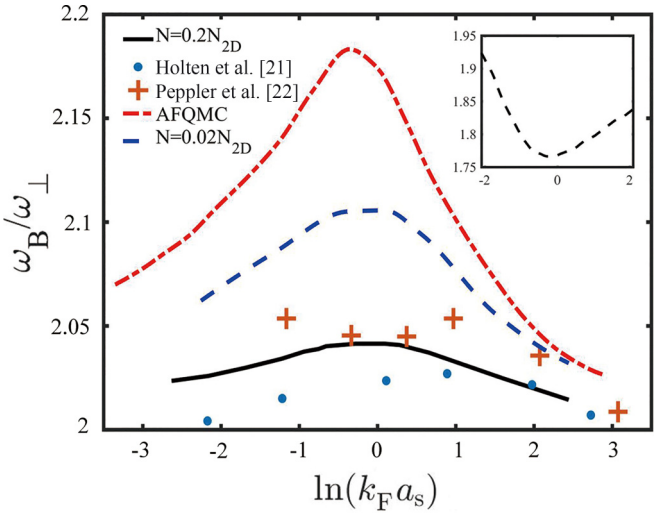

FIG. 4. Breathing-mode frequency change with the interaction $\ln(k_F a_s)$ of the systems for a different total number of atoms. The black solid line is the result of our dressed-molecule theory, the blue dots are the experimental data of Holten *et al.* [21] at $0.10 \sim 0.18T_F$, and the red pluses are the experimental data of Peppler *et al.* at $0.14 \sim 0.22T_F$ [22]; for these three data sets the total number $N/N_{2D} \sim 0.2$. The red dot-dashed line is the auxiliary-field quantum Monte Carlo (AFQMC) simulation data for $N/N_{2D} \to 0$ [37] and the blue dashed line is the result of our dressed-molecule theory for $N/N_{2D} = 0.02$. The inset shows the mean-field calculation of our dressed-molecule model at $N/N_{2D} = 0.2$.

the energy gap between the axial excited states and the axial ground state. This makes it that the axial excited-state fermions cannot be neglected even in the case of the particle number $N/N_{2D} = 0.2$. It should be noted that, even in the strong-interaction region, $|2\mu + |E_b|| \leqslant E_F \ll 1$ is also valid for the diluteness and the quasi-2D systems we consider, which makes the approximation of our dressed-molecule theory still effective. With the increase of the particle number, the proportion of the axial excited states will increase; the axial excited states will play an important role in the systems, which could make the breathing-mode frequency $\omega_B/\omega_\perp$ decrease. As these dressed states represent the three-dimensional properties in two-dimensional systems, the difference between the experimental data and the calculation of the QMC would become bigger for a larger number of particles. For our theory, as it covers the three types of states of the system, i.e., fermions in the axial ground state, fermions in axial excited states, and Feshbach molecular states, our calculation is in good agreement with the experimental results in the strong-interaction region even for a larger-number case.

In Fig. 4, which plots the breathing-mode frequency changing with the interaction of the systems compared to the experimental data and the QMC calculation, we show that our theory is a better low-energy effective theory as it can explain the experimental observations of the quantum anomaly for the whole BCS-BEC crossover, not only in the strong-interaction region [21,22,37]. At the BCS limit, the system can be considered as a noninteracting two-dimensional Fermi gas. The breathing-mode frequency ω_B must be twice $\omega_\perp$, which is the classical conclusion for the two-dimensional system; this phenomenon can be seen in our results or other data. As the system changes from the BCS limit to the resonance point, due to the effect of the axial excited-state fermions as explained above, the divergence between the experimental data and the QMC calculation becomes larger, which can be corrected in our theory. This divergence also existed in the previous two-dimensional polytropic fit and sum-rule results [2,4,38].

When the system enters the BEC part, the critical role of the fermions in terms of the properties of the system is replaced by the Feshbach molecules. This requires that the theory describing the quasi-2D system must include the properties of the Feshbach molecular states. Under this condition, the system can be approximately understood as a 3D one-component interacting Bose gas in a tight-binding harmonic trapping potential. This 3D molecular scattering length is $a^m_{3D} \simeq 0.6a_{3D}$ [33]. The energy shift between those Bose gases and the original Fermi system is $E_s \sim E_b$. In the BEC region, this energy shift cannot be neglected. This makes the effective models, which are based on the vacuum energy of the Fermi system, not applicable in this case. For our dressed-molecule theory, both the physics of 3D Feshbach molecular states and the effect of the energy shift are fully considered in the dressed-molecule model, so it can still describe the quasi-two-dimensional system well in the BEC region. In the BEC limit, it is equivalent to a quasi-2D weakly interacting BEC, for which the effective 2D molecular scattering length is

$$a^m_{2D} = \sqrt{\frac{\hbar^2\pi}{2m_f\omega_z\mathcal{B}}}\exp\left(-\sqrt{\frac{\hbar^2\pi}{4m_f\omega_z}}\frac{1}{a^m_{3D}}\right), \tag{30}$$

with $\mathcal{B} \simeq 0.905$ [31]. We can also get it from Eq. (8). For our dressed-molecule model, as discussed before, it can describe the physics around the bound-state energy well. At the limits $a_{3D} \to 0^+$ and $a^m_{2D} \to 0^+$, the interaction energy is far lower than the trap energy level, so the property of the system is a weak-interaction 2D Bose gas and the breathing-mode frequency $\omega_B/\omega_\perp$ will tend to 2. This phenomenon can be found from Fig. 4, especially our mean-field result. Therefore, we provide a theory that can better describe the quantum anomaly of the breathing mode in the whole BCS-BEC crossover process in an experimental system. We also plot $N/N_{2D} = 0.02$ in Fig. 4. Even in this case, there is still a big difference between our prediction and the dimensional QMC data. This shows that the experimental system cannot be described by a purely two-dimensional theory.

V. SUMMARY

We have developed a theory to describe the two-dimensional quantum anomaly of the breathing mode in an experimental system. Within our effective theory, the dressed molecules were used to characterize the axial excited-state fermions and the Feshbach molecules, which resulted in a good description of the high-dimensional effect in the strong-interaction region and the Feshbach molecular properties in the BEC part. On the other hand, with the aid of a beyond-mean-field Gaussian pair fluctuation theory, the quantum anomalous properties of the system could be explained. Our establishment of the dressed-molecule theory for 2D fermions

is crucial to the understanding of the conformal anomaly in the quasi-low-dimensional quantum systems and paves the way to investigate the quantum physics in other quasi-low-dimensional many-body systems.

ACKNOWLEDGMENTS

We thank Hui Hu, Wei Zhang, and Ke-Ji Chen for valuable discussions. F.W. was supported by National Youth Science Foundation of China (Grant No. 12204105), Educational Research Project for Young and Middle-Aged Teachers of Fujian Province (Grant No. JAT210041), and Natural Science Foundation of Fujian Province (Grant No. 2022J05116). L.H. was supported by National Key R&D Program (Grant No. 2018YFA0306503).

APPENDIX: QUASI-2D BUBBLE FUNCTION

Here we will prove that the two-particle bubble function for the three-dimensional two-component Fermi gases with s-wave interaction by a one-dimensional z-directional harmonic trap in this paper is equivalent to that in Petrov and Shlyapnikov's work [31]. From Eq. (9) we have

$$\begin{aligned} S_p(E) &= \sum_{m,n,\mathbf{k}} \gamma_{mn}^2\left(\mathcal{E}_{m,n,\mathbf{k}}^{-1}\right) + \sum_{\mathbf{k}} \frac{1}{2\epsilon_{\mathbf{k}}} \\ &= \sum_{n,i=(1\sim n),\mathbf{k}} \frac{[2-\delta(i)](2n-1)!!^2}{2^{2n}(2\pi)^{1/2}(n+i)!(n-i)!} \frac{1}{E-2\epsilon_{\mathbf{k}}-(1+2n)} + \sum_{\mathbf{k}} \frac{1}{2\epsilon_{\mathbf{k}}}. \end{aligned} \tag{A1}$$

By using the formula

$$\sum_{i=0}^{N} \frac{[2-\delta(i)](2N)!}{(2)^{2N}(N+i)!(N-i)!} = 1, \tag{A2}$$

the quasi-2D scattering amplitude can be written as

$$\begin{aligned} S_p(E) &= \sum_{n,\mathbf{k}} \frac{(2n-1)!!^2}{(2n)!(2\pi)^{1/2}} \frac{1}{E-2\epsilon_{\mathbf{k}}-(1+2n)} + \sum_{\mathbf{k}} \frac{1}{2\epsilon_{\mathbf{k}}} \\ &= \lim_{N\to\infty} \frac{1}{2(2\pi)^{3/2}} \left(\sum_{n=1}^{N} \frac{(2n-1)!!}{(2n)!!} \ln(n+\frac{1}{2}-E) - 2\sqrt{\frac{N}{\pi}}[\ln(N)-2] \right). \end{aligned} \tag{A3}$$

This is the quasi-2D bubble function in Petrov and Shlyapnikov's work [31]. Here S is the quantum area and m is the mass of the fermion. To complete this proof, we need to apply the formula

$$\sum_{n=0}^{N} \frac{(2n-1)!!}{(2n)!!} = \frac{2\Gamma\left(N+\frac{3}{2}\right)}{N!\sqrt{\pi}}. \tag{A4}$$

The proof is as follows. For the $N=0$ case we get

$$\sum_{n=0}^{0} \frac{(2n-1)!!}{(2n)!!} = 1 = 2\frac{1}{2}\frac{\sqrt{\pi}}{\sqrt{\pi}} = 2\frac{1}{2}\frac{\Gamma\left(\frac{1}{2}\right)}{\sqrt{\pi}} = 2\frac{\Gamma\left(N+\frac{3}{2}\right)}{N!\sqrt{\pi}}. \tag{A5}$$

So if for the $N=M-1$ case we have $\sum_{n=0}^{N} \frac{(2n-1)!!}{(2n)!!} = \frac{2\Gamma(N+3/2)}{N!\sqrt{\pi}}$ and for the $N=M$ case

$$\begin{aligned} \sum_{n=0}^{M} \frac{(2n-1)!!}{(2n)!!} &= \frac{2\Gamma\left(M+\frac{1}{2}\right)}{(M-1)!\sqrt{\pi}} + \frac{(2M-1)!!}{(2M)!!} \\ &= \frac{2\Gamma\left(M+\frac{1}{2}\right)}{(M-1)!\sqrt{\pi}} + \frac{\Gamma\left(M+\frac{1}{2}\right)}{\sqrt{\pi}(M)!} = \frac{2\Gamma\left(M+\frac{1}{2}\right)}{(M)!\sqrt{\pi}}\left(M+\frac{1}{2}\right) \\ &= \frac{2\Gamma\left(M+\frac{3}{2}\right)}{(M)!\sqrt{\pi}}, \end{aligned} \tag{A6}$$

we arrive at the conclusion that for any N we have $\sum_{n=0}^{N} \frac{(2n-1)!!}{(2n)!!} = \frac{2\Gamma(N+\frac{3}{2})}{N!\sqrt{\pi}}$. We also know that for the $N \gg 1$ case $\frac{\Gamma(N+\frac{3}{2})}{N!\sqrt{N}} \approx 1$. Combining these two equations, we arrive at the conclusion

$$\lim_{N\to\infty} \sum_{n=0}^{N} \frac{(2n-1)!!}{(2n)!!} = \frac{2\Gamma\left(N+\frac{3}{2}\right)}{N!\sqrt{\pi}} = \lim_{N\to\infty} 2\sqrt{\frac{N}{\pi}}. \tag{A7}$$

[1] W. A. Bardeen, Phys. Rev. **184**, 1848 (1969).
[2] J. Hofmann, Phys. Rev. Lett. **108**, 185303 (2012).
[3] P. A. Murthy, N. Defenu, L. Bayha, M. Holten, P. M. Preiss, T. Enss, and S. Jochim, Science **365**, 268 (2019).
[4] C. Gao and Z. Yu, Phys. Rev. A **86**, 043609 (2012).
[5] M. Olshanii, H. Perrin, and V. Lorent, Phys. Rev. Lett. **105**, 095302 (2010).
[6] M. Randeria, J.-M. Duan, and L.-Y. Shieh, Phys. Rev. Lett. **62**, 981 (1989).
[7] V. L. Berezinskii, Zh. Eksp. Teor. Fiz. **61**, 1144 (1971) [Sov. Phys. JETP **34**, 610 (1972)].
[8] J. M. Kosterlitz and D. J. Thouless, J. Phys. C **6**, 1181 (1973).
[9] J. Levinsen and M. M. Parish, in *Annual Review of Cold Atoms and Molecules*, edited by K. W. Madison, K. Bongs, L. D. Carr, A. M. Rey, and H. Zhai (World Scientific, Singapore, 2015), Vol. 3, Chap. 1, pp. 1–75.
[10] A. V. Turlapov and M. Y. Kagan, J. Phys.: Condens. Matter **29**, 383004 (2017).
[11] V. Makhalov, K. Martiyanov, and A. Turlapov, Phys. Rev. Lett. **112**, 045301 (2014).
[12] K. Martiyanov, T. Barmashova, V. Makhalov, and A. Turlapov, Phys. Rev. A **93**, 063622 (2016).
[13] K. Fenech, P. Dyke, T. Peppler, M. G. Lingham, S. Hoinka, H. Hu, and C. J. Vale, Phys. Rev. Lett. **116**, 045302 (2016).
[14] I. Boettcher, L. Bayha, D. Kedar, P. A. Murthy, M. Neidig, M. G. Ries, A. N. Wenz, G. Zürn, S. Jochim, and T. Enss, Phys. Rev. Lett. **116**, 045303 (2016).
[15] B. Fröhlich, M. Feld, E. Vogt, M. Koschorreck, W. Zwerger, and M. Kohl, Phys. Rev. Lett. **106**, 105301 (2011).
[16] A. T. Sommer, L. W. Cheuk, M. J. H. Ku, W. S. Bakr, and M. W. Zwierlein, Phys. Rev. Lett. **108**, 045302 (2012).
[17] Y. Zhang, W. Ong, I. Arakelyan, and J. E. Thomas, Phys. Rev. Lett. **108**, 235302 (2012).
[18] M. G. Ries, A. N. Wenz, G. Zürn, L. Bayha, I. Boettcher, D. Kedar, P. A. Murthy, N. Neidig, T. Lompe, and S. Jochim, Phys. Rev. Lett. **114**, 230401 (2015).
[19] P. A. Murthy, I. Boettcher, L. Bayha, M. Holzmann, D. Kedar, M. Neidig, M. G. Ries, A. N. Wenz, G. Zürn, and S. Jochim, Phys. Rev. Lett. **115**, 010401 (2015).
[20] E. Vogt, M. Feld, B. Fröhlich, D. Pertot, M. Koschorreck, and M. Köhl, Phys. Rev. Lett. **108**, 070404 (2012).
[21] M. Holten, L. Bayha, A. C. Klein, P. A. Murthy, P. M. Preiss, and S. Jochim, Phys. Rev. Lett. **121**, 120401 (2018).
[22] T. Peppler, P. Dyke, M. Zamorano, I. Herrera, S. Hoinka, and C. J. Vale, Phys. Rev. Lett. **121**, 120402 (2018).
[23] F. Wu, J. Hu, L. He, X.-J. Liu, and H. Hu, Phys. Rev. A **101**, 043607 (2020).
[24] R. Zhang, F. Wu, J.-R. Tang, G.-C. Guo, W. Yi, and W. Zhang, Phys. Rev. A **87**, 033629 (2013).
[25] Q. Chen, J. Stajic, S. Tan, and K. Levin, Phys. Rep. **412**, 1 (2005).
[26] J. P. Kestner and L.-M. Duan, Phys. Rev. A **74**, 053606 (2006).
[27] J. P. Kestner and L.-M. Duan, Phys. Rev. A **76**, 063610 (2007).
[28] W. Zhang, G.-D. Lin, and L.-M. Duan, Phys. Rev. A **77**, 063613 (2008).
[29] W. Zhang, G.-D. Lin, and L.-M. Duan, Phys. Rev. A **78**, 043617 (2008).
[30] W. Yi and L.-M. Duan, Phys. Rev. A **73**, 063607 (2006).
[31] D. S. Petrov and G. V. Shlyapnikov, Phys. Rev. A **64**, 012706 (2001).
[32] J. Hu, F. Wu, L. He, X.-J. Liu, and H. Hu, Phys. Rev. A **101**, 013615 (2020).
[33] L. He, H. Lv, G. Cao, H. Hu, and X.-J. Liu, Phys. Rev. A **92**, 023620 (2015).
[34] S. Stringari, Phys. Rev. A **58**, 2385 (1998).
[35] C. Menotti and S. Stringari, Phys. Rev. A **66**, 043610 (2002).
[36] H. Hu, G. Xianlong, and X.-J. Liu, Phys. Rev. A **90**, 013622 (2014).
[37] H. Shi, S. Chiesa, and S. Zhang, Phys. Rev. A **92**, 033603 (2015).
[38] U. Toniolo, B. C. Mulkerin, X.-J. Liu, and H. Hu, Phys. Rev. A **97**, 063622 (2018).